Applied Thermal Engineering 111 (2017) 8–19

Contents lists available at ScienceDirect

Applied Thermal Engineering

journal homepage: www.elsevier.com/locate/apthermeng

Research Paper

Thermodynamic analysis of a Kalina-based combined cooling and power cycle driven by low-grade heat source

Liyan Cao, Jiangfeng Wang *, Hongyang Wang, Pan Zhao, Yiping Dai

Institute of Turbomachinery, State Key Laboratory of Multiphase Flow in Power Engineering, School of Energy and Power Engineering, Xi'an Jiaotong University, Xi'an 710049, China

HIGHLIGHTS

- A Kalina-based combined cooling and power cycle is proposed to recover low-grade heat source.
- The effects of several parameters on cycle performance are examined.
- An optimization is conducted by GA to obtain optimum performance.

ARTICLE INFO

Article history:
Received 23 July 2016
Revised 24 August 2016
Accepted 16 September 2016
Available online 17 September 2016

Keywords:
Low-grade heat source
Kalina cycle
Absorption refrigeration cycle
Combined cooling and power
Optimization

ABSTRACT

This paper investigates a Kalina-based combined cooling and power (CCP) cycle driven by low-grade heat source. The proposed cycle consists of a Kalina cycle and an absorption refrigeration cycle. By establishing the mathematical model, numerical simulation is conducted and parametric analysis is performed to examine the effects of five key parameters on the thermodynamic performances of Kalina-based CCP cycle. A performance optimization is conducted by genetic algorithm to obtain the optimum exergy efficiency. According to parametric analysis, an optimum expander inlet pressure can be achieved; exergy efficiency increases with expander inlet pressure and concentration of ammonia-water basic solution, but exergy efficiency decreases when terminal temperature difference of high-temperature recuperator and low-temperature recuperator increases. Refrigeration exergy increases with expander inlet pressure and decreases as expander inlet temperature and concentration of ammonia-water basic solution rise. However, the refrigeration exergy keeps constant as the terminal temperature difference of high-temperature recuperator and low-temperature recuperator vary. Furthermore, the optimized Kalina-based CCP cycle is compared with a separate generation system which is also optimized. The optimization results show that the exergy efficiency and net power output of Kalina-based CCP are higher than those of separate generation system.

1. Introduction

In recent years, energy and environmental problems have increased interest in utilization of low-grade heat sources. Ammonia-water mixture is a low-boiling point working fluid, which exhibits favorable thermodynamic property in low-grade heat sources recovery. As a non-azeotropic mixture, ammonia-water mixture evaporates and condenses over a range of temperature. This characteristic of temperature glide enables the ammonia-water mixture to achieve a better temperature match between the working substance and the heat sources.

In 1984, Alexander Kalina [1] came up with a novel power cycle named Kalina cycle on the basis of ammonia-water mixture, in which a distiller condensate sub-system was innovatively proposed to solve the condensation problem of ammonia-water mixture at a relatively low turbine backpressure. Kalina cycle has the potential to accomplish efficient energy conversion of the low-grade heat sources. Mid/Low-temperature geothermal energy utilization with Kalina cycle drew researchers' attention, and Kalina cycle showed satisfactory thermodynamic performance [2–6]. In addition, Kalina cycle could be applied to solar energy utilization. Flat plate collector was usually chosen to boost Kalina cycle [7–9] owing to its low cost. However, the heat collecting temperature of flat plate collector is relatively low, the parabolic trough collector [10] and the compound parabolic collector [11] were employed to increase the heat collecting temperature.

Besides Kalina cycle, ammonia-water absorption refrigeration cycle was also expected to play a significant role in the low-grade heat source recovery. Researchers [12,13] conducted energy

* Corresponding author.
E-mail address: jfwang@mail.xjtu.edu.cn (J. Wang).

http://dx.doi.org/10.1016/j.applthermaleng.2016.09.088
1359-4311/

Nomenclature

E	exergy, kW
HRSG	heat recover steam generator
h	specific enthalpy, kJ·kg^{-1}
I	exergy destruction, kW
m	mass flow rate, kg·s^{-1}
P	pressure, MPa
Q	heat rate, kW
SHX	solution heat exchanger
s	specific entropy, kJ·(kg·K)$^{-1}$
T	temperature, K
t	temperature, °C
W	power, kW
x	ammonia mass fraction, %

Greek letters

η	efficiency
Δ	difference

Subscript

a	absorbent
abs	absorber
amb	ambient
b	ammonia-water basic solution
com	compressor
ex	exergy
exp	expander
gen	generator
HTR	high-temperature recuperator
in	inlet
isen	isentropic
LTR	low-temperature recuperator
net	net
out	outlet
p	ammonia-poor solution
pump	pump
r	ammonia-rich vapor
re	refrigerant
rec	rectifier
ref	refrigeration
s	strong solution
th	thermal

and exergy analysis for ammonia-water absorption refrigeration and found an optimum temperature of heat source to maximize the coefficiency of performance (COP) [14,15]. An experiment system has been established to verify the feasibility of ammonia-water absorption refrigeration cycle [15–17].

Nowadays, combined cooling and power cycle is a booming technology for efficient utilization of energy. Ammonia-water, which is widely used as working fluid in power cycle and refrigeration cycle, exhibits excellent thermodynamic performances. Therefore, many researchers have attempted to construct combined cooling and power cycles adopting ammonia–water as working fluid to improve overall energy conversion efficiency.

Zheng et al. [18] proposed a combined cooling and power cycle on the basis of Kalina cycle to generate power and refrigeration output simultaneously. The authors substituted the separator with rectifier to purify the ammonia vapor and inserted a condenser and an evaporator between the rectifier and the absorber. On this basis, Luo et al. [19] further analyzed combined cooling and power cycle proposed by Zheng. They conducted a sensitive analysis and mainly focus on the impact of the split ratio and the concentration of ammonia-water on cycle performance. Their results indicated that appropriate split ratio and concentration of ammonia-water could enable the cycle to satisfy the power and refrigeration demands of users. Sun et al. [20] combined a Rankine cycle with an absorption refrigeration cycle to generate power and refrigeration output by utilizing waste heat source. The high-temperature portion of the waste heat was used for power cycle, and the exhaust heat and low-temperature part were used to drive the refrigeration cycle. Their results showed that the combined cooling and power cycle was more efficient than separated power and refrigeration systems. The proposed combined cooling and power cycle only recover the heat carried by turbine exhaust. Besides, the turbine exhaust contained a certain amount of ammonia. In order to achieve heat and ammonia mass recovery, Sun et al. [21] modified their combined cooling and power cycle, in which the turbine exhaust was brought into the bottom of rectifier to act as the upward vapor in the process of rectification. Sun et al. combined the Rankine cycle with a single-effect refrigeration cycle. The single-effect absorption refrigeration system is the most commonly used design. But its coefficient of performance (COP) is relatively low comparing with double-effect refrigeration cycle. Therefore, researchers investigated the combination of power cycle and double-effect refrigeration cycle. Yu et al. [22] integrated a modified Kalina cycle and a double-effect absorption refrigeration cycle by mixing and splitting process to produce power and cooling. The flow rates could be adjusted by varying the split ratio, which enabled the cooling to power ratio to be adjustable. Jing and Zheng [23] coupled the Kalina cycle and the double-effect absorption refrigeration cycle as well. And they compared the coupled-configuration with the separated Kalina and double-effect absorption refrigeration cycle. The results showed that energy cascade utilization was enhanced by the coupled-configuration.

Zhang and Lior [24] came up with a parallel connected power and cooling cycle on the basis of absorption refrigeration cycle. The purified ammonia vapor was condensed and throttled down to produce refrigeration output in an evaporator. Meanwhile, the ammonia-poor solution absorbed heat in a boiler and expanded in a turbine. This cycle generated power and produced refrigeration in parallel, which took full advantage of ammonia-rich vapor and ammonia-poor solution, achieving cascade utilization of energy. Liu et al. [25] proposed a series connected ammonia-water refrigeration and power combined cycle. The ammonia-poor solution mixed with the ammonia-rich vapor in the absorber. And the mixture absorbed heat in the boiler and entered the turbine to expand. For the series connected cycle, the working fluid has higher ammonia concentration in heating process, which reduces the irreversibility of heating process. Based on the parallel connected and series connected combined cooling and power cycles, Liu and Zhang [26] proposed a concentration-adjustable combined cooling and power cycle by introducing splitting/absorption unit. In this cycle, the ammonia concentration increases in heat addition process and the decreases in absorption–condensation process. The irreversibility of both processes could be reduced simultaneously. Zhang and Lior [27] summarized the general principles for integration of power cycle and refrigeration cycle to achieve higher energy and exergy efficiencies.

As summarized above, the combined power and cooling cycles with excellent thermodynamic performance could generate power and cooling simultaneously. However, all these combined power

and cooling cycles were driven by relatively high temperature heat sources. For the low temperature heat sources including solar energy and geothermal energy, Goswami and Xu [28] innovatively proposed a new combined cooling and power cycle. This cycle showed potential to utilize the low grade heat sources. Goswami cycle [29] is the combination of the ammonia-water Rankine cycle and the absorption refrigeration cycle, in which the condenser and throttle valve were replaced by a turbine. Goswami cycle rapidly attracted researchers' attention, many researchers conducted thorough investigation on Goswami cycle from thermodynamic aspect. Hasan et al. [30] investigated the effect of heat source temperature on the performance of Goswami cycle from the thermal and exergy aspects. They found the existence of the optimum heat source temperature for second law efficiency. Lu and Goswami [31] examined the performance of Goswami cycle over a range of ambient temperature. The results showed that the first and second law efficiencies, power output, and refrigeration output declined as the ambient temperature rose. Kim et al. [32] conducted a performance assessment and examined the effect of some key parameters on the thermodynamic performance of Goswami cycle. Fontalvo et al. [33] performed an exergy analysis of Goswami cycle and found that the absorber, boiler and turbine contributed most to exergy destruction. In addition, the energy quality of power differed from that of refrigeration. For properly evaluating the thermodynamic performance of combined cycle, Vijayaraghavan and Goswami [34] developed several expressions for the first law, second law and exergy efficiency definitions based on the existing definitions in the literature. To accomplish efficient operation of Goswami cycle, researchers optimized the Goswami cycle to obtain the optimum parameter set. Demirkaya et al. [35] and Pouraghaie et al. [36] conducted a multi-objective optimization with Non-dominated Sorting Genetic Algorithm-II (NSGA-II). Work output, cooling capacity, effective first law and exergy efficiencies were selected as the objective function. To comprehensively evaluate the Goswami cycle, Zare et al. [37] took economic factors into consideration and established a thermoeconomic model. They carried out a parametric analysis to explore the effect of some key parameters on the thermoeconomic performance and conducted a thermoeconomic optimization of Goswami cycle. The optimization results indicated that economic performance was improved evidently. On the basis of sufficient theoretical investigation, Tamm and Goswami [38] constructed an experimental system. The experimental data basically agreed with simulation results, but there still appeared some deviations.

However, the amount of refrigeration capacity and refrigeration exergy generated by Goswami cycle was quite small, because the quality of turbine exhaust almost reached saturation state, which led to a small amount of evaporation capacity. Moreover, the amount of refrigeration capacity and refrigeration exergy was very sensitive to turbine performance [39]. Vidal et al. [40] investigated the impact of irreversibility in turbine on cycle performance in detail. They used the operation parameter reported in Ref. [30] and only changed the efficiencies of pump and turbine. They found that the temperature of turbine exhaust was higher than ambient temperature with turbine efficiency of 85%. At a given back pressure of turbine, the temperature of turbine exhaust increased as the turbine efficiency decreased, which could diminished the cooling effect. Then they lowered the back pressure of turbine to obtain proper temperature to produce refrigeration. However, the decrease in back pressure led to absorber temperature to be lower than ambient temperature. The absorption heat couldn't be rejected to environment. Generally, Goswami cycle had a relatively strict requirement for turbine efficiency, which restricted the adaptability of Goswami cycle to generate power and refrigeration by utilizing the low grade heat source under different condition. Above all, only the turbine with a large capacity can reach an isentropic efficiency up to 90%.

In order to improve the efficiency of combined cooling and power systems in low-grade heat recovery, a Kalina-based combined cooling and power (CCP) cycle is proposed. In Kalina cycle, the ammonia-poor solution is extracted from separator with a high temperature. It is potential to further utilize the heat contained by ammonia-poor solution. Thus, an absorption refrigeration cycle is inserted into Kalina cycle before the high-temperature recuperator to produce the power and refrigeration output simultaneously. And a parametric analysis is conducted to examine the effect of some key parameters on thermal and exergy efficiency. In order to verify that the proposed cycle has better performance, the Kalina-based combined cooling and power cycle is optimized by Genetic Algorithm and compared with a separate generation system under the same boundary condition. Moreover, an exergy destruction analysis under optimum condition is performed to investigate which component contributes most to overall cycle inefficiency.

2. System description

As shown in Fig. 1, the Kalina-based CCP cycle consists of a heat recover steam generator (HRSG), a separator, an expander, a generator, a high-temperature recuperator (HTR), a low-temperature recuperator (LTR), condenser I, pump I, throttle valve Iand an absorption refrigeration cycle. The absorption refrigeration cycle is made up of a distillation tower, condenser II, a precooler, throttle valve II, throttle valve III, an evaporator, an absorber, pump II and a solution heat exchanger (SHX). In this paper, an expander is used to generate power because expander has better adaptability for working medium comparing with turbine. There is no need to consider moisture content, oxygen content and impurities in working medium.

After being heated in HRSG, the ammonia-water basic solution in two-phase region is separated into ammonia-rich vapor and ammonia-poor solution in separator. The ammonia-rich vapor enters expander and expands to state 4. The ammonia-poor solution that possesses a relatively high temperature and mass flow rate serves as the heat source to drive the absorption refrigeration cycle. After releasing heat to absorption refrigeration cycle, the ammonia-poor solution is further cooled in HTR and is throttled down to a low pressure. Then the ammonia-poor solution is mixed with expander exhaust to form ammonia-water basic solution. The ammonia-water basic solution is cooled down to saturated state successively in low-temperature recuperator and condenser I. Then the ammonia-water basic solution is pressurized by pump I. The compressed ammonia-water basic solution absorbs heat in LTR and HTR in sequence. Afterwards, the ammonia-water basic solution enters the HRSG to finish the cycle.

For the absorption refrigeration cycle, the strong ammonia solution is pumped through SHX to distillation tower. The strong solution is heated by ammonia-poor solution in distillation tower and purified into refrigerant with high concentration. Then the refrigerant is condensed in condenser II, and the condensate is further cooled in precooler and is throttled down by throttle valve III, after which the temperature and pressure of refrigerant significantly drop. The low-temperature refrigerant releases its cold energy in evaporator. Then the refrigerant passes through the precooler and enters the absorber. In the distillation tower, the remaining ammonia weak solution, namely, absorbent is cooled and throttled into the absorber. The absorbent is mixed with the refrigerant to form strong ammonia solution. Meanwhile, the mixture is cooled by cooling water.

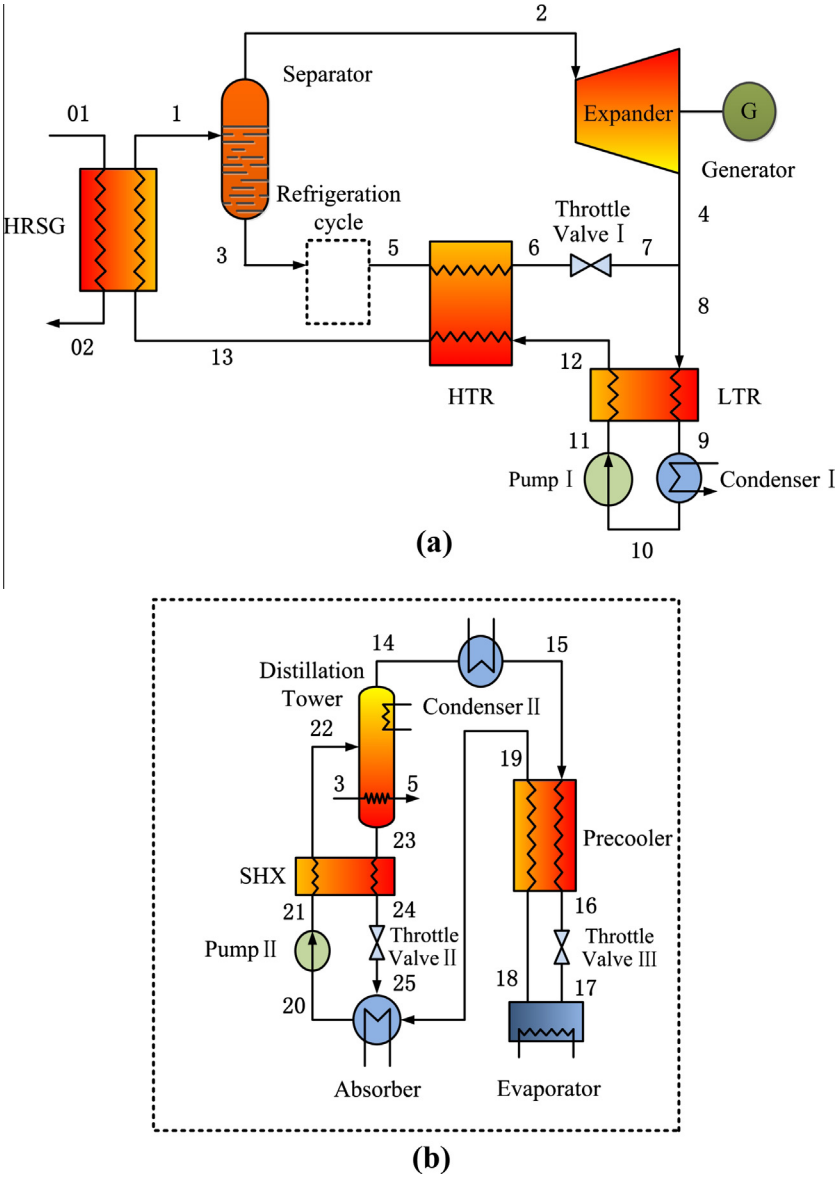

Fig. 1. Schematic diagram of Kalina-based CCP cycle.

3. Mathematical model

All the components in Kalina-based CCP cycle can be treated as control volume and the Kalina-based CCP cycle is modeled on mass and energy conservation. Some assumptions are made as follows to simplify the mathematical model:

(1) The cycle reaches a steady state. The potential and kinetic energy are neglected.
(2) The leakage of working fluid and pressure loss in pipes are neglected, while the pressure loss in some components cannot be neglected. In addition, the heat loss to ambient in all components and pipes are ignored.
(3) The isentropic efficiency of expander is a function of expansion ratio, and pumps have a given isentropic efficiency.
(4) The working fluid at absorber, condenser Iand condenser II outlet is saturated liquid.
(5) The flows across the throttle valve are isenthalpic.
(6) The refrigerant from distillation tower is saturated vapor and the absorbent from distillation tower is saturated liquid.

3.1. Energy and exergy analysis

The Kalina-based CCP cycle will be analyzed from energy and exergy perspective. Energy analysis based on the first law of thermodynamic discusses the energy conversion in quantity, but it is incapable of indicating the work potential or quality of different energy forms in relation to a given ambient condition [41]. Exergy method not only demonstrates the amount of usable work potential, or exergy, supplied as input to a system, but also reveals the system irreversibility distribution among different components and pinpoints the one contributing most to overall system inefficiency.

For heat exchangers including HRSG, HTR, LTR, SHX, precooler, condensers and so on, the mass and energy balance equation take the forms

$$m_{\mathrm{in},1} + m_{\mathrm{in},2} = m_{\mathrm{out},1} + m_{\mathrm{out},2} \tag{1}$$

$$m_{\mathrm{in},1} h_{\mathrm{in},1} + m_{\mathrm{in},2} h_{\mathrm{in},2} = m_{\mathrm{out},1} h_{\mathrm{out},1} + m_{\mathrm{out},2} h_{\mathrm{out},2} \tag{2}$$

The exergy destruction equation of the heat exchangers can be represented as

$$I = E_{in,1} + E_{in,2} - E_{out,1} - E_{out,2} \tag{3}$$

For condensers, the cooling water will not be further utilized after condensing the working fluid in the cycle, the exergy destruction equation of condensers becomes

$$I = E_{in} - E_{out} \tag{4}$$

Exergy is calculable as $E = m[(h - h_{amb}) - T_{amb}(s - s_{amb})]$.

The isentropic efficiency of expander is given by

$$\eta_{exp} = \frac{h_{in} - h_{out}}{h_{in} - h_{out,isen}} \tag{5}$$

The expander power output is

$$W_{exp} = m(h_{in} - h_{out}) \tag{6}$$

The exergy destruction equation of expander is as follows

$$I = E_{in} - E_{out} - W_{exp} \tag{7}$$

For separator, the mass balance equation, ammonia mass balance equation and energy balance equation can be expressed as

$$m_b = m_r + m_p \tag{8}$$

$$m_b x_b = m_r x_r + m_p x_p \tag{9}$$

$$m_{in} h_{in} = m_{out,1} h_{out,1} + m_{out,2} h_{out,2} \tag{10}$$

The exergy destruction equation of separator is

$$I = E_{in} - E_{out,1} - E_{out,2} \tag{11}$$

Mass balance equation, ammonia mass balance equation and energy balance equation of absorber are as follows

$$m_s = m_{re} + m_a \tag{12}$$

$$m_s x_s = m_{re} x_{re} + m_a x_a \tag{13}$$

$$m_{out,1} h_{out,1} + Q_{abs} = m_{in,1} h_{in,1} + m_{in,2} h_{in,2} \tag{14}$$

where Q_{abs} is the heat of absorption.

The exergy destruction equation of absorber is written as

$$I = E_{in,1} + E_{in,2} - E_{out} \tag{15}$$

For distillation tower, the mass balance equation, ammonia mass balance equation and energy balance equation of absorber are

$$m_s = m_{re} + m_a \tag{16}$$

$$m_s x_s = m_{re} x_{re} + m_a x_a \tag{17}$$

$$m_{in} h_{in} + Q_{gen} = m_{out,1} h_{out,1} + m_{out,2} h_{out,2} + Q_{rec} \tag{18}$$

where Q_{gen} is heat of generator in distillation tower and Q_{rec} is heat of rectifier in distillation tower.

The exergy destruction equation of distillation tower can be represented as

$$I = E_{in,1} + E_{in,2} - E_{out,1} - E_{out,2} - E_{out,3} \tag{19}$$

The isentropic efficiency of pumps is defined as

$$\eta_{pump} = \frac{h_{out,isen} - h_{in}}{h_{out} - h_{in}} \tag{20}$$

The work input by pumps can be written as

$$W_{pump} = m(h_{out} - h_{in}) \tag{21}$$

The exergy destruction equation of pumps is

$$I = E_{in} + W_{pump} - E_{out} \tag{22}$$

According to assumption (5), the flows across the throttle valve are isenthalpic, thus the energy balance equation and exergy destruction equation of valves are

$$h_{in} = h_{out} \tag{23}$$

$$I = E_{in} - E_{out} \tag{24}$$

In this work, the thermal efficiency and exergy efficiency are adopted to evaluate the cycle performance. The thermal efficiency can be defined as the useful energy output divided by energy input from heat source [6], given by

$$\eta_{th} = \frac{W_{net} + Q_{ref}}{Q_{in} - Q_{out}} \tag{25}$$

Using exergy change of heat source as exergy input to cycle, exergy efficiency becomes [6]

$$\eta_{ex} = \frac{W_{net} + E_{ref}}{E_{in} - E_{out}} \tag{26}$$

The net power output of the cycle is defined as

$$W_{net} = W_{exp} - W_{pump,1} - W_{pump,2} \tag{27}$$

3.2. Mathematical model validation

To verify the validity of the mathematical model, the available data in literature serves as contrast to the simulation results. The Kalina cycle and absorption refrigeration cycle are validated by data in Ref. [42] and Ref. [12], respectively. The Kalina cycle has the similar schematic diagram as illustrated in Fig. 1(a). When refrigeration cycle isn't attached to Kalina cycle, state 3 and state 5 are the same point. Therefore, all node numbers of Kalina cycle is in conformity with those in Fig. 1(a) and state 3 and state 5 share the same thermodynamic parameters. Each point of absorption refrigeration cycle corresponds to those in Fig. 1(b).

The validation results are presented in Tables 1 and 2, in which the simulation results are well consistent with the data in literature.

4. Result and discussion

In this section, a parametric analysis for Kalina-based CCP cycle driven by low-temperature exhaust gas is performed and an optimization is also conducted to investigate the optimum thermodynamic performance of Kalina-based CCP cycle. All the thermodynamic properties of ammonia-water mixture are calculated by REFPROP 9.1 developed by the National Institute of Standard and Technology of the United States. On the basis of mathematical model, the numerical simulation is implemented by MATLAB software. The boundary condition and simulation parameters for Kalina-based CCP cycle are summarized in Table 3. The pressure loss of some components is listed in Table 4. The isentropic efficiency curve of expander over expansion ratio provided by expander manufacturer is illustrated in Fig. 2. The isentropic efficiency curve of expander is embedded in the simulation program. And all restricted conditions of expander are shown in Table 5.

4.1. Parametric analysis

Before thermodynamic optimization, a parametric analysis is conducted for Kalina-based CCP cycle to examine the effect of five key thermodynamic parameters on the cycle performance. These parameters include expander inlet pressure P_2, expander inlet temperature t_2, concentration of basic solution x_b, terminal

Table 1
Mathematical model validation for Kalina cycle; (a) present work, (b) Ref. [42].

State	t (°C)		P (MPa)		x (%)		m (kg·s^{-1})	
	(a)	(b)	(a)	(b)	(a)	(b)	(a)	(b)
1	116.00	116.00	3.23	3.23	82.00	82.00	16.60	17.16
2	116.00	116.00	3.23	3.23	96.61	97.00	11.47	11.52
3	116.00	116.00	3.23	3.23	49.36	51.00	5.13	5.65
4	44.10	41.30	0.66	0.66	96.61	97.00	11.47	11.52
5	116.00	116.00	3.23	3.23	49.36	51.00	5.13	5.65
6	45.07	45.29	3.13	3.13	49.36	51.00	5.13	5.65
7	45.42	45.29	0.66	0.66	49.36	51.00	5.13	5.65
8	45.42	45.29	0.66	0.66	82.00	82.00	16.60	17.16
9	29.32	29.90	0.559	0.56	82.00	82.00.	16.60	17.16
10	8.00	8.00	0.46	0.48	82.00	82.00	16.60	17.16
11	8.42	8.44	3.53	3.53	82.00	82.00	16.60	17.16
12	40.07	40.29	3.43	3.43	82.00	82.00	16.60	17.16
13	61.95	62.87	3.33	3.33	82.00	82.00	16.60	17.16

Table 2
Mathematical model validation for refrigeration cycle; (a) present work, (b) Ref. [12].

State	t (°C)		P (MPa)		x (%)		m (kg·s^{-1})	
	(a)	(b)	(a)	(b)	(a)	(b)	(a)	(b)
14	45.05	44.07	1.56	1.56	99.96	99.96	0.13	0.14
15	40.00	40.00	1.56	1.56	99.96	99.96	0.13	0.14
16	16.55	16.88	1.56	1.56	99.96	99.96	0.13	0.14
17	−15.11	−14.14	0.24	0.25	99.96	99.96	0.13	0.14
18	−10.00	−10.00	0.24	0.25	99.96	99.96	0.13	0.14
19	37.39	37.39	0.24	0.25	99.96	99.96	0.13	0.14
20	40.00	40.00	0.24	0.25	35.44	37.09	1.06	1.00
21	40.44	40.45	1.56	1.56	35.44	37.09	1.06	1.00
22	111.80	110.06	1.56	1.56	35.44	37.09	1.06	1.00
23	130.00	130.31	1.56	1.56	26.45	27.09	0.93	0.86
24	40.44	40.45	1.56	1.56	23.45	27.09	0.93	0.86
25	40.70	40.71	0.24	0.25	23.45	27.09	0.93	0.86

Table 3
The boundary condition and simulation condition for Kalina-based CCP cycle.

Term	Value
Heat source	Exhaust gas (26.80%N_2, 73.20% CO_2)
Mass flow rate of heat source	20.00 kg/s
Temperature of heat source	140.00 °C
Pressure of heat source	500.00 kPa
Ambient temperature	20.00 °C
Ambient pressure	101.30 kPa
Expander inlet pressure	3000.00 kPa
Expander inlet temperature	120.00 °C
Concentration of basic solution	70.00%
Terminal temperature difference of HTR	10.00 °C
Terminal temperature difference of LTR	10.00 °C
Pump efficiency [42]	60.00%
Pinch-point temperature difference	10.00 °C
Terminal temperature difference of heat exchanger	5.00 °C
Concentration of refrigerant	99.96%
Refrigerating temperature	0.00 °C

Table 4
Pressure loss for components [43,44].

Term	Value
Pressure loss in HRSG	40.00 kPa
Pressure loss in HTR	80.00 kPa
Pressure loss in LTR	50.00 kPa
Pressure loss in condenser I	80.00 kPa
Pressure loss in distillation tower	20.00 kPa
Pressure loss in condenser II	10.00 kPa
Pressure loss in precooler	20.00 kPa
Pressure loss in absorber	10.00 kPa
Pressure loss in SHX	10.00 kPa
Pressure loss in evaporator	10.00 kPa

temperature difference of HTR Δt_{HTR} and terminal temperature difference of LTR Δt_{LTR}. In the parametric analysis, as one parameter is examined, others are kept constant as listed in Table 3.

Fig. 3 depicts the influence of expander inlet pressure on exergy efficiency, thermal efficiency, net power output, refrigeration capacity and refrigeration exergy. As the expander inlet pressure increases, the specific enthalpy drop in expander rises. However, an increase in expander inlet pressure leads to a decrease in mass flow rate of ammonia-rich vapor separated from separator. It turns out that the net power output increases first and then decreases. Meanwhile, the ammonia-poor solution goes up which leads to

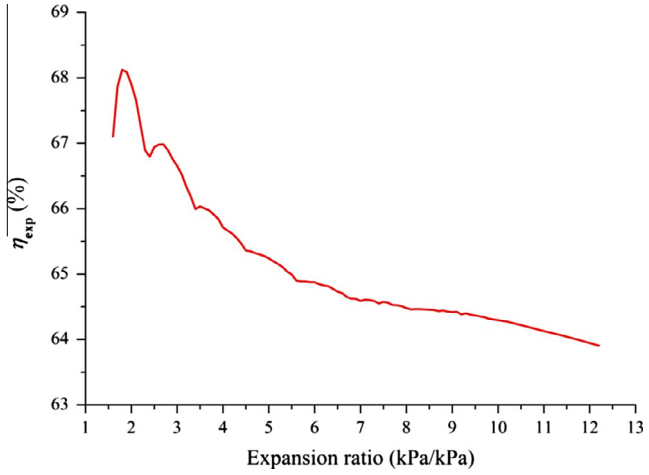

Fig. 2. Isentropic efficiency of expander over expansion ratio.

Table 5
Restricted conditions of expander.

Term	Value
Maximum expander inlet pressure	4000.00 kPa
Maximum expander inlet temperature	300.00 °C
Maximum expansion ratio	12.20

an increase in the heat offered to absorption refrigeration cycle. The mass flow rate of refrigerant is positively correlated with the heat offered to absorption refrigeration cycle. As a consequence, the refrigeration capacity and the refrigeration exergy increase with the mass flow rate of refrigerant. The value of net power output is much greater than that of refrigeration exergy. Therefore, the refrigeration exergy scarcely imposes influence on the exergy efficiency. As a result, the exergy efficiency shares the same variation trend with net power output. The thermal efficiency increases with expander inlet pressure. This is because the values of net power and refrigeration capacity share the same order of magnitudes, thus, both of net power and refrigeration capacity have influence on thermal efficiency. Even more important, the reduction in the mass flow rate of ammonia-rich vapor is greater than the growth of mass flow rate of ammonia-poor solution, which leads to a decrease in mass flow rate of ammonia-water basic solution. Consequently, energy input from heat source drops as the mass flow rate of ammonia-water basic solution decreases. Under the comprehensive impact of net power output, refrigeration capacity and energy input, the thermal efficiency increases with expander inlet pressure.

Fig. 4 illustrates the effect of expander inlet temperature on exergy efficiency, thermal efficiency, net power output, refrigeration capacity and refrigeration exergy. As the expander inlet temperature increases, the specific enthalpy drop in expander increases. However, an increase in expander inlet temperature leads to the drop of mass flow rate of ammonia-water basic solution. The mass flow rate of ammonia-rich vapor and ammonia-poor solution decreases as well. Under the combined influence of reduction in mass flow rate of ammonia-rich vapor and the growth of specific enthalpy drop in expander, the net power output increases first and then goes down slightly. As the mass flow rate of ammonia-poor solution decreases, the heat offered to absorption refrigeration cycle goes down. Therefore, the mass flow rate of refrigerant generated from distillation tower declines, which leads to the drop of refrigeration capacity and refrigeration exergy. Comparing with the refrigeration exergy, the net power output exerts greater impact over exergy output. Furthermore, the reduction in mass flow rate of ammonia-water basic solution leads to a decrease in exergy input. Thus, the exergy efficiency increases with expander inlet temperature. For thermal efficiency, the decrement of refrigeration capacity far exceeds the increment of power output, which leads to a significant drop of energy output. As a consequence, the thermal efficiency decreases.

Fig. 5 shows the effect of concentration of ammonia-water basic solution on exergy efficiency, thermal efficiency, net power output, refrigeration capacity and refrigeration exergy. As the concentration of ammonia-water basic concentration increases, the mass flow rate of ammonia-rich vapor goes up and the mass flow rate of ammonia-poor solution goes down. The net power output is mainly determined by the mass flow rate of ammonia-rich vapor. Therefore, the net power output increases with the concentration of ammonia-water basic solution. And the decrease in mass flow rate of ammonia-poor solution leads to a reduction in the heat offered to absorption refrigeration cycle. As a result, the mass flow rate of refrigerant decreases, and the refrigeration capacity and the refrigeration exergy fall simultaneously. The net power output is the dominant factor in exergy output comparing with the refrigeration exergy and exerts great influence over exergy efficiency. Therefore, the exergy efficiency increases with concentration of ammonia-water basic solution. The thermal efficiency shows a downtrend when the concentration of ammonia-water basic solution rises. This is because the refrigeration capacity shares the same order of magnitudes with net power output and declines markedly, which leads to a reduction in energy output. As a result, the thermal efficiency decreases.

Fig. 6 presents the effect of terminal temperature difference of HTR on the exergy efficiency, thermal efficiency, net power output, refrigeration capacity and refrigeration exergy. The terminal temperature difference of HTR has no impact on refrigeration capacity and refrigeration exergy. Therefore, the refrigeration capacity and refrigeration exergy keep constant as the terminal temperature difference of HTR increases. The terminal temperature difference of HTR is also irrelevant to net power output, so the net power output remained unchanged as well. The amount of heat conduction through HTR decreases when the terminal temperature difference of HTR increases. And the HTR outlet temperature of ammonia-water basic solution falls accordingly. That's to say, the average

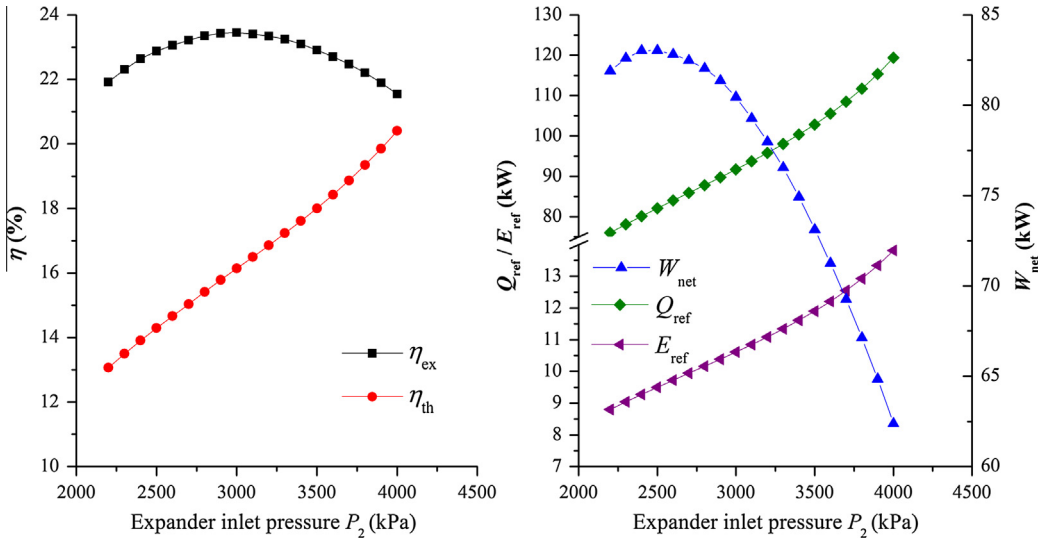

Fig. 3. Effect of expander inlet pressure on exergy efficiency, thermal efficiency, net power output, refrigeration capacity and refrigeration exergy.

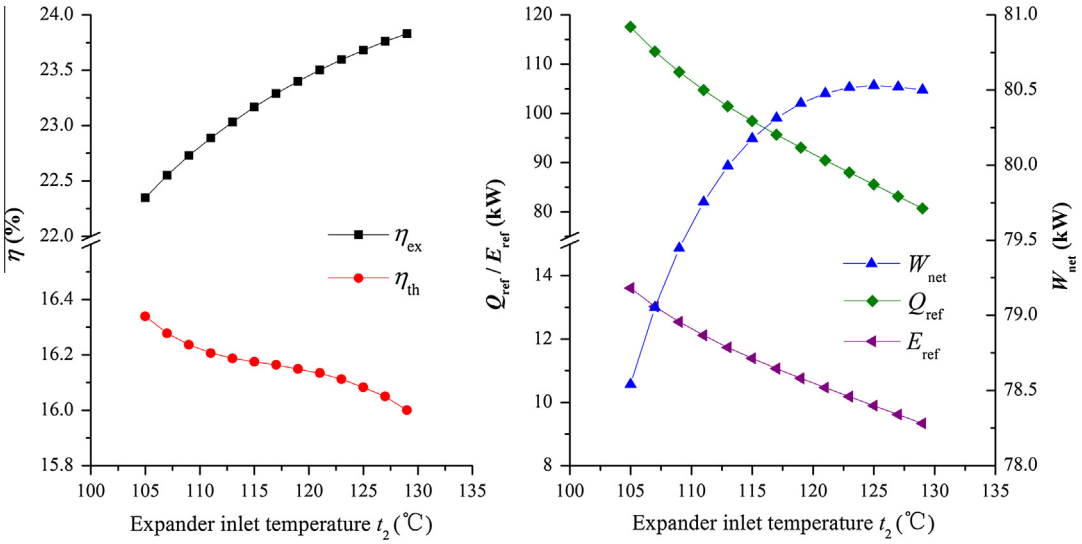

Fig. 4. Effect of expander inlet temperature on exergy efficiency, thermal efficiency, net power output, refrigeration capacity and refrigeration exergy.

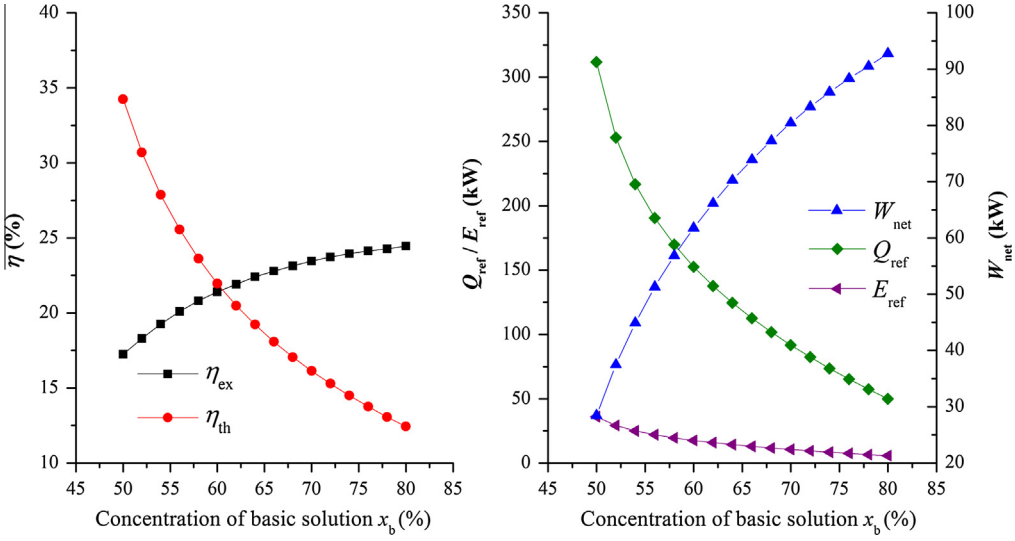

Fig. 5. Effect of concentration of ammonia-water basic solution on exergy efficiency, thermal efficiency, net power output, refrigeration capacity and refrigeration exergy.

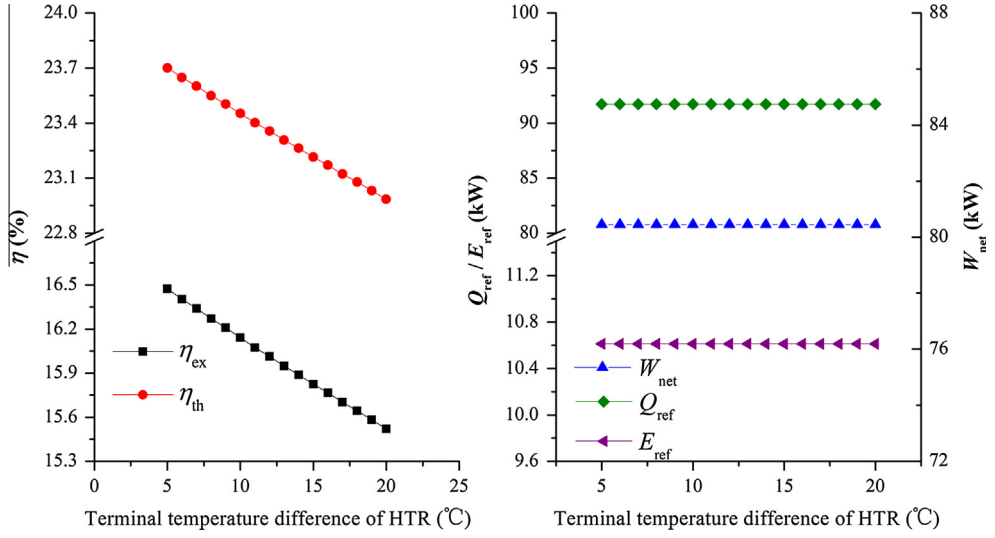

Fig. 6. Effect of terminal temperature difference of HTR on the exergy efficiency, thermal efficiency, net power output, refrigeration capacity and refrigeration exergy.

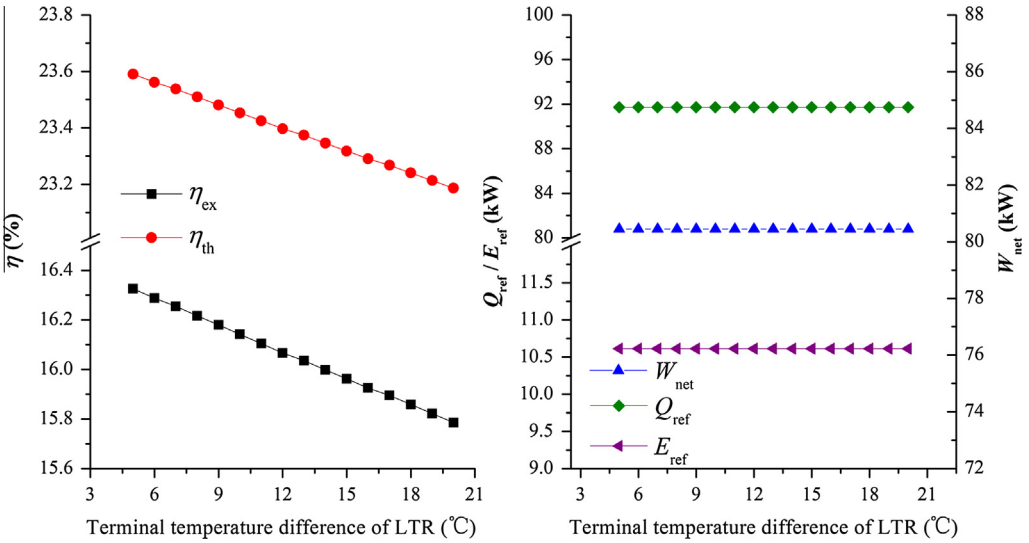

Fig. 7. Effect of terminal temperature difference of LTR on the exergy efficiency, thermal efficiency, net power output, refrigeration capacity and refrigeration exergy.

temperature of heat addition decreases, which leads to an increase in energy input and exergy input from heat source. As a consequence, the exergy efficiency and thermal efficiency decreases simultaneously.

Fig. 7 displays the effect of terminal temperature difference of LTR on exergy efficiency, thermal efficiency, net power output, refrigeration capacity and refrigeration exergy. The terminal temperature difference of LTR is unrelated to net power output, refrigeration capacity and refrigeration exergy. Thus, the net power output, refrigeration capacity and refrigeration exergy all remain constant. For exergy efficiency and thermal efficiency, as the terminal temperature difference of LTR increases, the LTR outlet temperature of ammonia-water basic solution falls. And the HTR outlet temperature of ammonia-water basic solution decreases as well, which leads to an increase in energy input and exergy input from heat source. Therefore, the exergy efficiency and thermal efficiency decreases when the terminal temperature difference of LTR increases.

4.2. Optimization and comparison

According to the parametric analysis, it is necessary to conduct an optimization for Kalina-based CCP cycle to obtain the optimum thermodynamic performance. Genetic Algorithm is employed to optimize the Kalina-based CCP cycle. Genetic Algorithm [45] was initially proposed by Holland. It is a stochastic global search method which is inspired by the process of natural selection. Genetic Algorithm is superior to traditional optimization techniques because it involves a search from a population of solutions rather than a single point, and it has better global optimization capability. The genetic algorithm encodes a potential solution to a specific domain problem on a chromosome-like data structure, in which where genes are parameters of the problem to be solved. Genetic Algorithm conducts evolution search without any external information, and fitness function is the only criterion to evaluate the adaptability of an individual. The individual with low adaptability will be eliminated. Selection operator, crossover operator and mutation operator are the basic operators of Genetic Algorithm. The selection operator selects parents for next generation of solutions. The individual with higher fitness has higher probability to be selected. The crossover operator produces new chromosomes. It produces new individuals that have some parts of both parent's genetic material. The mutation operator randomly modifies values in the chromosomes with low probability. At each generation, Genetic Algorithm selects the individuals according to their fitness in the problem domain, and produces new populations of solution with the help of crossover and mutation operator. This process leads to evolution of populations that are better suited to the environment.

In the process of optimization, the exergy efficiency is selected as the objective function for Kalina-based CCP cycle. Three key thermodynamic parameters including expander inlet pressure P_2, expander inlet temperature t_2, concentration of basic solution x_b are chosen as the decision variables. According to the parametric analysis, the lower terminal temperature difference of HTR and LTR are, the higher the exergy efficiency is. The effect of terminal temperature difference of HTR and LTR on exergy efficiency is predictable. Therefore, terminal temperature difference of HTR and LTR will not be optimized. The terminal temperature difference of HTR and LTR are 5 °C in optimization.

In this paper, an absorption refrigeration cycle is attached to Kalina cycle to recover heat from ammonia-poor solution before the HTR. In order to investigate how this addition affects the cycle performance, a comparison between the Kalina-based CCP cycle and a system for separate generation of power and refrigeration is conducted under the optimum operation condition. The separate generation system that consists of a Kalina cycle and a compression refrigeration cycle driven by the Kalina cycle is illustrated in Fig. 8. The separate generation system is optimized to achieve maximum exergy efficiency under the condition that the separate generation system generates the same amount of refrigeration exergy with Kalina-based CCP cycle. And the definition of exergy efficiency for separate generation system takes the form of Eq. (26), but the net power output of separate generation system is given by

$$W_{net} = W_{exp} - W_{com} - W_{pump} \tag{28}$$

where W_{com} is power consumption of compressor.

The expander inlet pressure P_2, expander inlet temperature t_2, concentration of basic solution x_b, are chosen as the decision variables. In addition, R134a is chosen as the working fluid for the compression refrigeration cycle [46].

The Kalina-based CCP cycle shares the same boundary and optimization condition with separate generation system. The operation parameters of Genetic Algorithm and ranges of key thermodynamic parameters for both systems are listed in Table 6. Further-

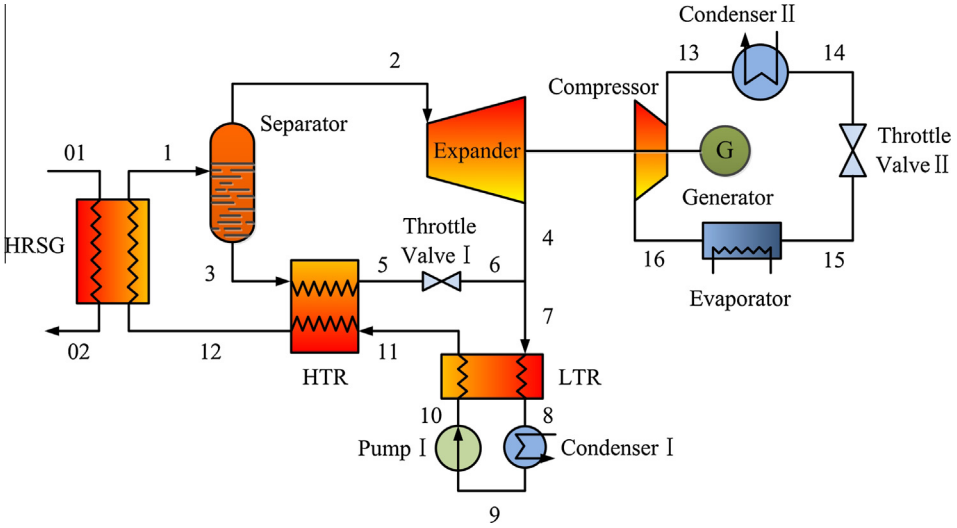

Fig. 8. Separate generation system for power and refrigeration.

Table 6
Operation parameters for optimization.

Term	Value
Population size	100
Generation	100
Ranges of expander inlet pressure	1600–4000 kPa
Ranges of expander inlet temperature	100–140 °C
Ranges of concentration of basic solution	50–80%

more, some restricts have to be set in the optimization program. For example, all restricted conditions for expander is listed in Table 5; the pinch-point temperature difference is the minimum temperature difference in process of evaporation; the degassing width between concentration of strong solution and concentration of absorbent shouldn't be lower than 0.6 [44]; the basic solution heated by HRSG should be in two-phase region; in all heat exchangers, the temperature of hot fluid shouldn't be lower than that of cold fluid. The thermodynamic parameters of each point

Table 8
Optimization results for Kalina-based CCP cycle and separate generation system.

Term	Kalina-based CCP cycle	Separate generation system
Expander inlet pressure	3571.85 kPa	3517.29 kPa
Expander inlet temperature	129.57 °C	129.77 °C
Concentration of basic solution	80.00%	80.00%
Exergy efficiency	25.76%	23.44%
Net power output	89.59 kW	77.81 kW
Power consumption of compressor	/	12.54 kW
Refrigeration exergy	5.58 kW	5.58 kW

Table 7
Thermodynamic parameters of each point for Kalina-based CCP cycle under optimum condition.

State	t (°C)	P (kPa)	x (%)	h (kJ·kg^{-1})	s kJ·(kg·K)$^{-1}$	m (kg·s^{-1})	Quality
1	129.57	3571.85	80.00	1460.50	4.81	0.980	0.70
2	129.57	3571.85	94.64	1852.56	5.88	0.690	1.00
3	129.57	3571.85	45.18	528.01	2.28	0.290	0.00
4	76.34	905.30	94.64	1712.29	6.09	0.690	0.95
5	77.70	3551.85	45.18	264.60	1.58	0.290	0.00
6	71.24	3471.85	45.18	232.32	1.49	0.290	0.00
7	66.63	905.30	45.18	232.32	1.50	0.290	0.02
8	71.57	905.30	80.00	1274.23	4.73	0.980	0.68
9	51.05	855.30	80.00	1069.82	4.14	0.980	0.59
10	25.00	775.30	80.00	250.27	1.48	0.980	0.00
11	26.01	3741.85	80.00	257.36	1.49	0.980	0.00
12	66.24	3691.85	80.00	461.77	2.13	0.980	0.00
13	68.09	3611.85	80.00	471.32	2.16	0.980	0.00
14	32.84	1012.62	99.96	1650.79	5.87	0.040	1.00
15	25.00	1002.62	99.96	461.60	1.88	0.040	0.00
16	11.64	982.62	99.96	398.49	1.67	0.040	0.00
17	−9.59	295.56	99.96	398.49	1.69	0.040	0.08
18	−5.00	285.56	99.96	1605.33	6.28	0.040	1.00
19	20.00	265.56	99.96	1668.44	6.54	0.040	1.00
20	25.00	255.56	44.42	−4.54	0.76	0.133	0.00
21	25.36	1032.62	44.42	−3.04	0.76	0.133	0.00
22	75.70	1022.62	44.42	309.19	1.71	0.133	0.04
23	124.57	1012.62	20.50	475.71	1.90	0.093	0.00
24	30.36	1002.62	20.50	29.04	0.62	0.093	0.00
25	30.48	265.56	20.50	29.04	0.62	0.093	0.00
01	140.00	500.00	/	476.95	5.77	20.000	1.00
02	92.36	460.00	/	428.51	5.66	20.000	1.00

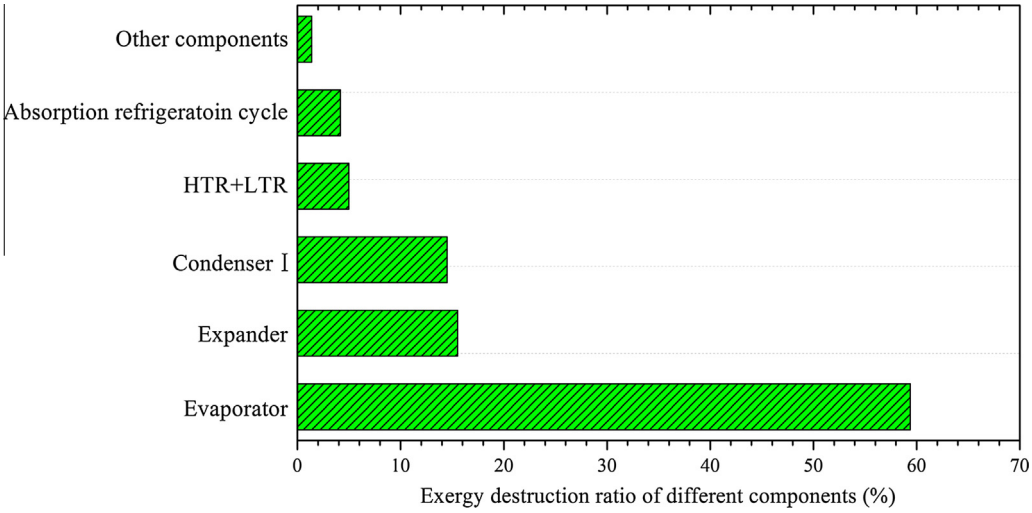

Fig. 9. Exergy destruction ratio of different components.

for Kalina-based CCP cycle under optimum condition are listed in Table 7. And optimization results for Kalina-based CCP cycle and separate generation system are summarized in Table 8.

As shown in Table 7, the optimization results are highly consistent with the parametric analysis for Kalina-based CCP cycle. Under the optimum condition, the exergy efficiency for Kalina-based CCP cycle is 25.76%. The net power output and refrigeration exergy are 89.59 kW and 5.58 kW, respectively. For separate generation system, the optimum exergy efficiency is 23.44%, which is lower than that of Kalina-based CCP cycle by 2.32%. As for net power output, separate generation system generates 77.81 kW power and it is 11.78 kW lower than that of Kalina-based CCP cycle. The compressor in separate generation system consumes 12.54 kW power to generate the same amount of refrigeration exergy with Kalina-based CCP cycle.

4.3. Exergy destruction of different components

Fig. 9 illustrates the exergy destruction ratio of different components in Kalina-CCP cycle at the optimum condition. It can be seen that the exergy destruction caused by HRSG is about 59.49% owing to the irreversibility in heat transfer at the relatively high temperature, which contributes most to overall exergy destruction. Thus, HRSG needs careful design and selection. And the exergy destruction of expander and condenser I are 15.61% and 14.41%, respectively. For HTR and LTR, exergy destruction is 4.89%. The exergy destruction caused by absorption refrigeration cycle is only 4.12%, this is because the mass flow rate of absorption refrigeration cycle is relatively small comparing with that of Kalina cycle. And the exergy destroyed by remaining components is less than 2%.

5. Conclusion

In this paper, a Kalina-based CCP cycle driven by low-grade heat source is analyzed. By establishing mathematical model, a simulation is conducted to perform parametric analysis. Five key parameters including expander inlet pressure, expander inlet temperature, concentration of ammonia-water basic solution, terminal temperature difference of HTR and terminal temperature difference of LTR are selected to explore their effects on the thermodynamic performances of Kalina-based CCP cycle. According to the parametric analysis, an optimization is conducted by Genetic Algorithm to search for optimum exergy efficiency. Moreover, a comparison between Kalina-based CCP cycle and separate generation system is conducted under the optimum condition. The main conclusions are summarized as follows:

(1) Exergy efficiency increases with expander inlet temperature and concentration of ammonia-water basic solution; exergy efficiency decreases as the terminal temperature difference of HTR and LTR increases. An optimum expander inlet pressure can be achieved to maximize exergy efficiency.
(2) Refrigeration exergy is positively correlated with mass flow rate of refrigerant. The mass flow rate of refrigerant rises with expander inlet pressure, which leads to an increase in refrigeration exergy. As the expander inlet temperature and concentration of ammonia-water basic solution increases, the mass flow rate of refrigerant and refrigeration exergy decline simultaneously. The terminal temperature difference of HTR and LTR are irrelevant with refrigeration exergy.
(3) Comparing the optimization results of Kalina-based CCP cycle and separate generation system, Kalina-based CCP cycle has higher exergy efficiency and generates more net power output than separate generation system does on the condition that the Kalina-based CCP cycle and separate generation system produce the same amount of refrigeration exergy.
(4) Exergy analysis of Kalina-based CCP cycle at the optimum condition illustrates that the HRSG contributes most exergy destruction to the cycle, which is the largest source of overall cycle inefficiency. And expander and condenser I destroy second largest amount of exergy. The exergy destruction of absorption refrigeration cycle is relatively small on account of small mass flow rate of working fluid.

Acknowledgements

The authors gratefully acknowledge the financial support by the National Natural Science Foundation of China (Grant No. 51476121) and the Fundamental Research Funds for the Central Universities (Grant No. 2013jdgz14).

References

[1] A.I. Kalina, Combined-cycle system with novel bottoming cycle, J. Eng. Gas Turb. Power-Trans. ASME 106 (4) (1984) 737–742.

[2] H. Saffari, S. Sadeghi, M. Khoshzat, P. Mehregan, Thermodynamic analysis and optimization of a geothermal Kalina cycle system using Artificial Bee Colony algorithm, Renewable Energy 89 (2016) 154–167.
[3] M. Fallah, S. Mohammad, S. Mahmoudi, M. Yari, R.A. Ghiasi, Advanced exergy analysis of the Kalina cycle applied for low temperature enhanced geothermal system, Energy Convers. Manage. 108 (2016) 190–201.
[4] Nasruddin, R. Usvika, M. Rifaldi, A. Noor, Energy and exergy analysis of Kalina cycle system (KCS) 34 with mass fraction ammonia-water mixture variation, J. Mech. Sci. Technol. 23 (7) (2009) 1871–1876.
[5] W. Fu, J. Zhu, T. Li, W. Zhang, J. Li, Comparison of a Kalina cycle based cascade utilization system with an existing organic Rankine cycle based geothermal power system in an oilfield, Appl. Therm. Eng. 58 (1–2) (2013) 224–233.
[6] M. Yari, Exergetic analysis of various types of geothermal power plants, Renewable Energy 35 (1) (2010) 112–121.
[7] F. Sun, Y. Ikegami, H. Arima, W. Zhou, Performance analysis of the low-temperature solar-boosted power generation system-Part I: Comparison between Kalina solar system and rankine solar system, J. Sol. Energy Eng.-Trans. ASME 135 (1) (2013).
[8] F. Sun, Y. Ikegami, H. Arima, W. Zhou, Performance analysis of the low temperature solar-boosted power generation system-Part II: Thermodynamic characteristics of the Kalina solar system, J. Sol. Energy Eng.-Trans. ASME 135 (1) (2013).
[9] S. Faming, Z. Weisheng, K. Nakagami, S. Xuanming, Energy-economic analysis and configuration design of the Kalina solar-OTEC system, Int. J. Comput. Electr. Eng. 5 (2) (2013) 187–191.
[10] M. Ashouri, A.M.K. Vandani, M. Mehrpooya, M.H. Ahmadi, A. Abdollahpour, Techno-economic assessment of a Kalina cycle driven by a parabolic Trough solar collector, Energy Convers. Manage. 105 (2015) 1328–1339.
[11] J.F. Wang, Z.Q. Yan, E.M. Zhou, Y.P. Dai, Parametric analysis and optimization of a Kalina cycle driven by solar energy, Appl. Therm. Eng. 50 (1) (2013) 408–415.
[12] S.A. Adewusi, S.M. Zubair, Second law based thermodynamic analysis of ammonia-water absorption systems, Energy Convers. Manage. 45 (15–16) (2004) 2355–2369.
[13] J. Koehler, W.J. Tegethoff, D. Westphalen, M. Sonnekalb, Absorption refrigeration system for mobile applications utilizing exhaust gases, Heat Mass Transfer 32 (5) (1997) 333–340.
[14] X.H. Wu, B. Chen, D.X. Zheng, Thermodynamic analysis of ammonia-water absorption refrigeration cycle, J. North China Electr. Power Univ. 30 (5) (2003) 66–69.
[15] J. Fernandez-Seara, M. Vazquez, Study and control of the optimal generation temperature in NH_3-H_2O absorption refrigeration systems, Appl. Therm. Eng. 21 (3) (2001) 343–357.
[16] A.A. Manzela, S.M. Hanriot, L. Cabezas-Gomez, J.R. Sodre, Using engine exhaust gas as energy source for an absorption refrigeration system, Appl. Energy 87 (4) (2010) 1141–1148.
[17] R. Best, J. Hernandez, Experimental studies on the operating characteristics of an ammonia water-absorption system for solar cooling, Chem. Eng. Res. Des. 69 (2) (1991) 153–160.
[18] D.X. Zheng, B. Chen, Y. Qi, H.G. Jin, Thermodynamic analysis of a novel absorption power/cooling combined-cycle, Appl. Energy 83 (4) (2006) 311–323.
[19] C.D. Luo, N. Zhang, R.X. Cai, M. Liu, Sensitivity analysis of ammonia absorption power/refrigeration combined cycle, Proc. CSEE 28 (17) (2008) 1–7.
[20] L. Sun, W. Han, X. Jing, D. Zheng, H. Jin, A power and cooling cogeneration system using mid/low-temperature heat source, Appl. Energy 112 (2013) 886–897.
[21] L. Sun, W. Han, D. Zheng, H. Jin, Assessment of an ammonia-water power/cooling cogeneration system with adjustable solution concentration, Appl. Therm. Eng. 61 (2) (2013) 443–450.
[22] Z. Yu, J. Han, H. Liu, H. Zhao, Theoretical study on a novel ammonia-water cogeneration system with adjustable cooling to power ratios, Appl. Energy 122 (2014) 53–61.
[23] X. Jing, D. Zheng, Effect of cycle coupling-configuration on energy cascade utilization for a new power and cooling cogeneration cycle, Energy Convers. Manage. 78 (2014) 58–64.
[24] N. Zhang, N. Lior, Development of a novel combined absorption cycle for power generation and refrigeration, J. Energy Resour. Technol.-Trans. ASME 129 (3) (2007) 254–265.
[25] M. Liu, N. Zhang, R.X. Cai, Series connected ammonia-water refrigeration and power combined cycle and its sensitivity analysis, Proc. CSEE 26 (1) (2006) 1–7.
[26] M. Liu, N. Zhang, Proposal and analysis of a novel ammonia-water cycle for power and refrigeration cogeneration, Energy 32 (6) (2007) 961–970.
[27] N. Zhang, N. Lior, Methodology for thermal design of novel combined refrigeration/power binary fluid systems, Int. J. Refrig. 30 (6) (2007) 1072–1085.
[28] D.Y. Goswami, F. Xu, Analysis of a new thermodynamic cycle for combined power and cooling using low and mid temperature solar collectors, J. Sol. Energy Eng.-Trans. ASME 121 (2) (1999) 91–97.
[29] F. Xu, D.Y. Goswami, S.S. Bhagwat, A combined power/cooling cycle, Energy 25 (3) (2000) 233–246.
[30] A.A. Hasan, D.Y. Goswami, S. Vijayaraghavan, First and second law analysis of a new power and refrigeration thermodynamic cycle using a solar heat source, Sol. Energy 73 (5) (2002) 385–393.
[31] S.G. Lu, D.Y. Goswami, Optimization of a novel combined power/refrigeration thermodynamic cycle, J. Sol. Energy Eng.-Trans. ASME 125 (2) (2003) 212–217.
[32] K.H. Kim, G. Kim, C.H. Han, Performance assessment of ammonia-water based power and refrigeration cogeneration cycle, Int. J. Mater. Mech. Manuf. 1 (1) (2013) 36–40.
[33] A. Fontalvo, H. Pinzon, J. Duarte, A. Bula, A. Gonzalez Quiroga, Padilla R. Vasquez, Exergy analysis of a combined power and cooling cycle, Appl. Therm. Eng. 60 (1–2) (2013) 164–171.
[34] S. Vijayaraghavan, D.Y. Goswami, On evaluating efficiency of a combined power and cooling cycle, Trans. ASME J. Energy Resour. Technol. 125 (3) (2003) 221–227.
[35] G. Demirkaya, S. Besarati, R. Vasquez Padilla, A. Ramos Archibold, D.Y. Goswami, M.M. Rahman, et al., Multi-objective optimization of a combined power and cooling cycle for low-grade and midgrade heat sources, J. Energy Resour. Technol.-Trans. ASME 134 (3) (2012).
[36] M. Pouraghaie, K. Atashkari, S.M. Besarati, N. Nariman-Zadeh, Thermodynamic performance optimization of a combined power/cooling cycle, Energy Convers. Manage. 51 (1) (2010) 204–211.
[37] V. Zare, S.M.S. Mahmoudi, M. Yari, M. Amidpour, Thermoeconomic analysis and optimization of an ammonia-water power/cooling cogeneration cycle, Energy 47 (1) (2012) 271–283.
[38] G. Tamm, D.Y. Goswami, Novel combined power and cooling thermodynamic cycle for low temperature heat sources, part II: Experimental investigation, J. Sol. Energy Eng.-Trans. ASME 125 (2) (2003) 223–229.
[39] R. Vasquez Padilla, G. Demirkaya, D.Y. Goswami, E. Stefanakos, M.M. Rahman, Analysis of power and cooling cogeneration using ammonia-water mixture, Energy 35 (12) (2010) 4649–4657.
[40] A. Vidal, R. Best, R. Rivero, J. Cervantes, Analysis of a combined power and refrigeration cycle by the exergy method, Energy 31 (15) (2006) 3401–3414.
[41] T.J. Kotas, The Exergy Method of Thermal Plant Analysis, Anchor Brendon Ltd, Tiptree, Essex, Great Britain, 1985.
[42] V. Zare, S.M.S. Mahmoudi, M. Yari, On the exergoeconomic assessment of employing Kalina cycle for GT-MHR waste heat utilization, Energy Convers. Manage. 90 (2015) 364–374.
[43] V. Zare, S.M.S. Mahmoudi, M. Yari, Ammonia–water cogeneration cycle for utilizing waste heat from the GT-MHR plant, Appl. Therm. Eng. 48 (2012) 176–185.
[44] S.W. Yang, Basic theory and design of ammonia-water absorption refrigeration system: thermodynamic calculation, Fluid Eng. 5 (1990) 55–63.
[45] Y.P. Dai, J.F. Wang, L. Gao, Parametric optimization and comparative study of organic Rankine cycle (ORC) for low grade waste heat recovery, Energy Convers. Manage. 50 (3) (2009) 576–582.
[46] Y.Z. Wu, Principles of Refrigeration and Cryogenic Technology, Higher Education Press, Beijing, 2004.